Feasibility study on lengthening the high-voltage cable section and reducing the number of cable joints via alternative bonding methods

Li, Mingzhen; Zhou, Chengke; Zhou, Wenjun; Zhang, Jun; Zhang, Liang; Yao, Leiming

Published in:
High Voltage

DOI:
10.1049/hve.2019.0011

Publication date:
2019

Document Version
Publisher's PDF, also known as Version of record

High Voltage

Research Article

IET Journals
The Institution of Engineering and Technology

Feasibility study on lengthening the high-voltage cable section and reducing the number of cable joints via alternative bonding methods

eISSN 2397-7264
Received on 24th January 2019
Revised 29th April 2019
Accepted on 11th June 2019
doi: 10.1049/hve.2019.0011
www.ietdl.org

Mingzhen Li[1], Chengke Zhou[1,2] ✉, Wenjun Zhou[1], Jun Zhang[3], Liang Zhang[3], Leiming Yao[3]

[1]School of Electrical Engineering and Automation, Wuhan University, No. 299, Bayi Road, Wuchang District, Wuhan, People's Republic of China

[2]School of Engineering and Built Environment, Glasgow Caledonian University, Cowcaddens Road, Glasgow, UK

[3]State Grid Jiangsu Electric Power Company, State Grid Corporation of China, No. 555, Laodong Road, Gusu District, Suzhou, People's Republic of China

✉ *E-mail: C.Zhou@gcu.ac.uk*

Abstract: Among all failures in cable circuits, the failure rate of cable joints is much higher than that in cable bodies. In an effort to reduce cable failure rates and improve the reliability of power cable systems, this article studies the possibility of increasing the length of a cable section and thus reducing the number of cable joints via alternative sheath bonding methods. As the maximum length of an electrical cable section is governed by the permissible sheath standing voltage, this article first proposes a precise sheath voltage calculation model without approximations and simplifications. The sheath voltage per unit length has then been calculated for each bonding method using the proposed model. The maximum length of a cable section has then been calculated, based on the permissible sheath standing voltage, for the various sheath bonding methods. Results show that the traditional 500-m minor section length could be increased to 2.21 km by using the single-point bonding method. The maximum distance can be further lengthened by increasing the physical spacing among the three-phase cables. The economic comparison for each bonding method has also been made. Finally, the proposed method has been applied to a HV cable circuit already in operation, and the operational data confirms the feasibility.

1 Introduction

High-voltage (HV) cables are more widely used in urban power distribution systems in recent years, for the improvement in aesthetics and higher reliability [1–3]. With the rapid growth of HV cables, the number of cable failures has increased [2, 3]. The failure rate of cable joints was reported to be ∼4 times higher than that in cable bodies, based on HV cable failure statistics [4–6], and cable joints (accessories) are known to be the main source of insulation weakness in HV cables. In addition, cable circuit failures contributed to a big proportion of customer lost minutes.

A cable joint is used to connect two cable sections. Unlike the cable bodies, cable joints are assembled and installed on site by skilled workers. Up to 24 man-hours are required to install a single cable joint in a HV line [5]. There is a series of processes that require very high levels of human-skill and which could be impacted by environmental conditions. Any little imperfection in the processes can result in premature failure of the joint. Therefore, the unreliability of HV cable system is mainly caused by human factors.

Many studies have investigated and reported on the design of cable bodies or cable joints [7–9], aiming to improve the performance of the conductor and the insulation. Some studies contributed to the analysis of cable joint internal overheating problems [10–12], which can lead to the improvement of the cable joint design scheme. There have also been simulations or experimental studies of cable joint defects [13–15], which facilitated characteristics of various defects and made the condition diagnosis easier. However, cable joints are still the weakest links in a cable system. Efforts are needed to improve the reliability of HV cable system.

In order to improve the reliability of HV cable systems, this paper aims at studying the possibility of lengthening a HV cable section and reducing the number of cable joints, by using single-point bonding or middle-point bonding instead of the traditional cross-bonding method. Since the maximum length of an electrical cable section is governed by the permissible sheath standing voltage at the isolated end, this paper first propose a precise sheath voltage calculation model, one which does without approximations and simplifications. Second, calculation of the maximum length of a typical HV cable section using both single-point bonding and middle bonding methods is carried out, and the economics of each bonding method is analysed. Finally, the proposed method is validated against a HV cable circuit already in operation.

The maximum electrical length of a cable section can be defined as the cable length that causes the sheath voltage at the isolated end to reach the maximum permissible standing voltage. It is to be noted that the practical limitation for the maximum length of a cable section is the available transportation equipment, especially for land transportation, however, this belongs to another subject category. The goal of the paper is to determine the maximum electrical length.

2 Description of the sheath bonding methods

The selection of sheath bonding method depends on the length of the cable circuit. Cross bonding and single-point bonding have been the most widely applied bonding methods.

Long HV cable circuits (>1.2 km) are recommended to have their metal sheath or the conductors transposed [16–18] every 400–500 m. As shown in Fig. 1, the interchanging of the earthing arrangement is known as the cross bonding system. In addition to the six cable terminals (three-phase) at the two ends of the HV cable, where the sheaths are grounded, there are six cable joints within a major section of an HV cable. A major section, as shown in the figure, is expected to be 1200–1500 m long.

There are also other bonding techniques for the metal sheath of HV cables, such as single-point bonding, multiple single-point bonding, impedance bonding etc. Single-point bonding is the simplest and most effective method of sheath bonding, as shown in Fig. 2. The maximum length of the cable section is governed by the permissible sheath standing voltage at the isolated (protected) end.

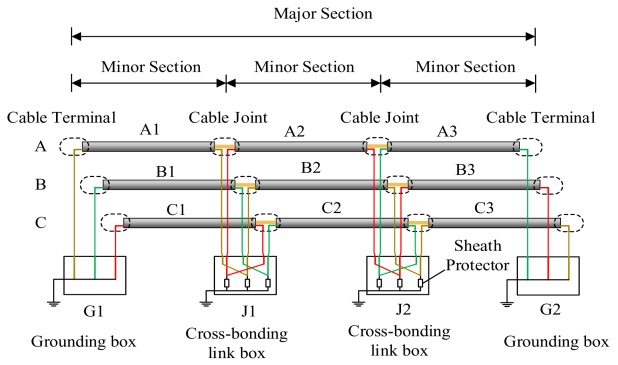

Fig. 1 *Configuration of a major section of a cross bonded HV cable system*

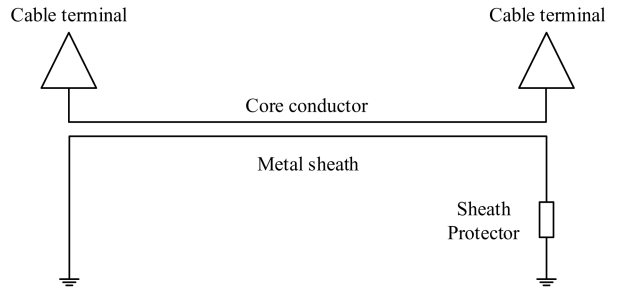

Fig. 2 *Configuration of a single-point bonded HV cable system*

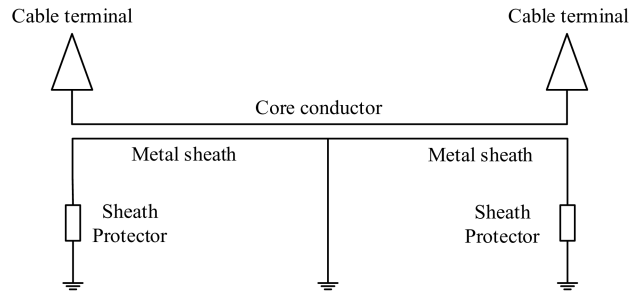

Fig. 3 *Configuration of a middle -point bonding HV cable system*

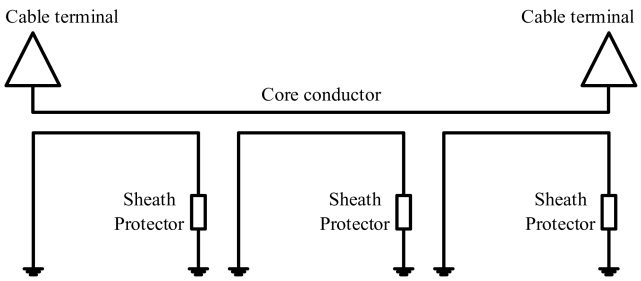

Fig. 4 *Configuration of a multiple single-point bonding HV cable system*

Power companies usually have strict regulations on the maximum allowed level of the sheath voltage [19], and the cable length can be determined by the regulations. Usually, if the length of a single-point bonding section is <800 m, no cable joint is needed in this cable section.

When the cable length is such that the sheath-standing voltage limit is exceeded when the ground is connected at one end of the circuit, the ground connection may be shifted along the circuit run. In Fig. 3, for example, the earth bonding point is in the centre of the cable length, this is called 'middle-point bonding'. Usually, if the middle-point bonding section has a length of 800–1200 m, just three cable joints (one for each of the three-phases) are needed in the cable circuit.

For long cable circuits, another solution is to use sheath sectionalising joints (multiple single-point bonding shown in Fig. 4) so that the sheath standing voltage for each minor section is within the limit imposed. In practice, the cross bonding system is always preferred to the multiple single-point bonding method, because a parallel ground continuity conductor (GCC) is needed in single-point bonding, middle-point bonding and multiple single-point bonding systems in case of a ground fault [17]. The parallel GCC gives a return path for the zero-sequence current, while also adds appreciably to the cost of the cable system.

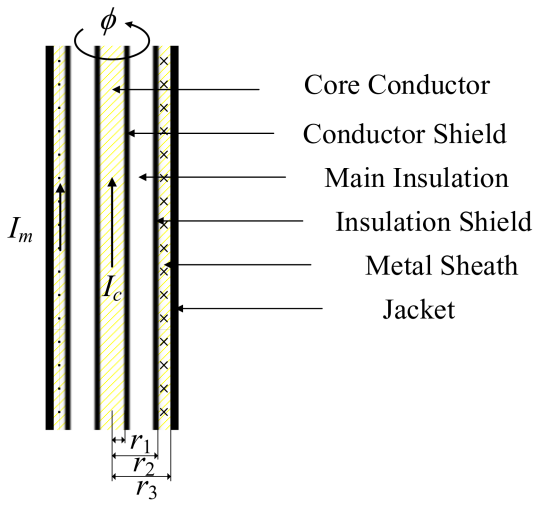

Fig. 5 *Longitudinal section of a typical HV cable*

3 Sheath voltage calculation model

The sheath voltage is mainly induced from the core current of the cable line itself and the current of nearby circuits.

The factors affecting sheath voltage induced from the core current can be presented in Fig. 5, where I_m represents the sheath current, and I_c represents the core current, r_1 represents the core radius, r_2 represents the outer radius of main insulation, and r_3 represents the outer radius of metal sheath. The magnetic induction of the metal sheath comes from both I_m and I_c, represented as $B_s(I_m)$ and $B_s(I_c)$. The magnetic induction can be calculated by Ampere's circuital law, i.e., the integral of the magnetic induction B around a closed path C equals the magnetic permeability μ times the current crossing the area bounded by C. When a circle of radius r ($r_2 < r < r_3$) is chosen to be the closed path, the current enclosing the circle area is $(r^2 - r_2^2)/(r_3^2 - r_2^2) \cdot I_m$. The equation of $B_s(I_m)$ is presented as (1)

$$B_s(I_m) = \frac{\mu_0 (r^2 - r_2^2) I_m}{2\pi (r_3^2 - r_2^2) r}. \tag{1}$$

The magnetic flux of the metal sheath $\Phi_s(I_m)$ is the integral of B_s, which can be presented as (2)

$$\Phi_s(I_m) = \int_{r_2}^{r_3} \frac{\mu_0 (r^2 - r_2^2)}{2\pi (r_3^2 - r_2^2) r} I_m dr = \frac{\mu_0 I_m}{2\pi} \left(\frac{1}{2} - \frac{r_2^2}{r_3^2 - r_2^2} \ln \frac{r_3}{r_2} \right). \tag{2}$$

It is to be noted that the flux linkage $\Psi_s(I_m)$ linking with the current inside the closed path can be represented as (3)

$$\begin{aligned} \Psi_s(I_m) &= \int_{r_2}^{r_3} \frac{\mu_0 (r^2 - r_2^2)^2}{2\pi (r_3^2 - r_2^2)^2 r} I_m dr \\ &= \mu_0 I_m \left(\frac{r_3^2 - 3r_2^2}{8(r_3^2 - r_2^2)} + \frac{r_2^4}{2\pi (r_3^2 - r_2^2)^2} \cdot \ln \frac{r_3}{r_2} \right). \end{aligned} \tag{3}$$

According to Faraday's law of electromagnetic induction, the induced electromotive force of the core conductor per unit length is given as (4)

$$e_s(I_m) = -\frac{d\Psi_s}{dt}. \tag{4}$$

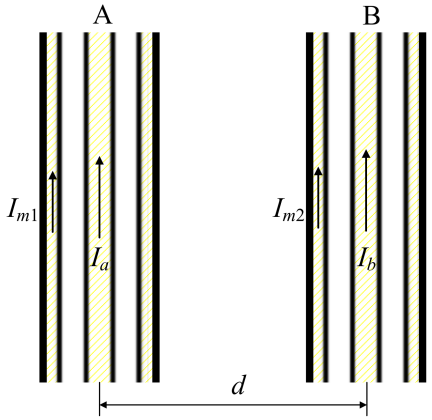

Fig. 6 *Configuration of the induced voltage from the current of nearby circuits*

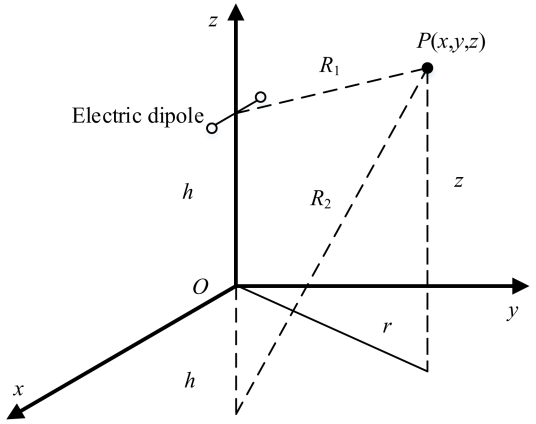

Fig. 7 *Configuration of a pair of horizontal electric dipoles with the observation point P*

Assuming $i_m(t)=I_{AM}\cdot\sin(\omega t+\theta)$, where I_m is the phasor form of $i_m(t)$; I_{AM} is the amplitude of $i_m(t)$; ω is the angular frequency of $i_m(t)$, $\omega=2\pi f$; f is the frequency of $i_m(t)$; t is time variable; θ is time constant. Then the phasor form of $e_s(I_m)$ can be written as (5)

$$E_s(I_m)=-j\mu_0 f\left(\frac{r_3^2-3r_2^2}{4\left(r_3^2-r_2^2\right)}+\frac{r_2^4}{\left(r_3^2-r_2^2\right)^2}\cdot\ln\frac{r_3}{r_2}\right)\cdot I_m. \tag{5}$$

Similarly, the equation of the magnetic induction $B_s(I_c)$, the flux linkage $\Psi_s(I_c)$, and the induced electromotive force $E_s(I_c)$ can be represented as in (6)–(8), respectively

$$B_s(I_c)=\frac{\mu_0 I_c}{2\pi r}. \tag{6}$$

$$\Psi_s(I_c)=\int_{r_2}^{r_3}B_s(I_c)\mathrm{d}r=\frac{\mu_0 I_c}{2\pi}\ln\frac{r_3}{r_2}. \tag{7}$$

$$E_s(I_c)=-j\mu_0 f\ln\frac{r_3}{r_2}\cdot I_c. \tag{8}$$

The sheath voltage induced from the current of nearby circuits can be shown in Fig. 6, where I_{m1} represents the sheath current of phase A cable, I_{m2} represents the sheath current of phase A cable, I_a represents the core current of phase A cable, I_b represents the core current of phase B cable, and d represents the distance between phase A cable and phase B cable. In this case, Ampere's circuital law cannot be easily used to calculate the induced voltage from the current of nearby circuits, because no apparent closed path C can be selected to encircle the current circuit. However, the theory of electric dipole [20] and Sommerfeld integral [21] can be used for the calculation. The current element can be treated as a pair of electric dipoles, as shown in Fig. 7, and the electric dipole is above the ground with the height of h, the distance between the electric dipole and the observation point P is R_1, the distance between the observation point P and the mirror of the electric dipole is R_2.

In an infinite space of non-conducting medium, the component of the Hertz electric vector Π generated at the observation point $P(x, y, z)$ of the electric dipole orientation is presented in (9)

$$\Pi=-\frac{j\omega\mu I\mathrm{d}x}{4\pi k^2}\frac{e^{jkR_1}}{R_1}. \tag{9}$$

$$R_1=\sqrt{x^2+y^2+(h-z)^2} \tag{10}$$

$$\frac{e^{jkR_1}}{R_1}=\int_0^\infty\frac{u}{\sqrt{u^2-k^2}}e^{-\sqrt{u^2-k^2}|h-z|}J_0(ru)\mathrm{d}u. \tag{11}$$

$$k=j\sqrt{j\omega\mu(\sigma+j\omega\varepsilon)}. \tag{12}$$

$$r=\sqrt{x^2+y^2}. \tag{13}$$

Equation (11) is called the Sommerfeld integral, where k represents the medium propagation constant, $J_0(ru)$ represents 0-order Bessel function of the first kind, u represents the spatial frequency, r represents the horizontal distance between the electric dipole and the observation point. Assuming plane xOy is the interface between the air (above xOy) and the earth (under xOy), the Hertz electric vector in the air can be shown in (14), and the Hertz electric vector in the earth can be shown in (15). The horizontal component of each electric field strength observed in the air and the earth are (17) and (18), respectively. The sheath voltage per unit length is the sum of $E_s(I_m)$, $E_s(I_c)$ and (E_a or E_e)

$$\Pi_a=-\frac{j\omega\mu I\mathrm{d}x}{4\pi k_0^2}\left[\frac{e^{jk_0R_1}}{R_1}-\frac{e^{jk_0R_2}}{R_2}+2\int_0^\infty\frac{u}{\beta_0+\beta_1}e^{-\beta_0(z+h)}J_0(ru)\mathrm{d}u\right]. \tag{14}$$

$$\Pi_e=-\frac{j\omega\mu I\mathrm{d}x}{4\pi k_0^2}\int_0^\infty\frac{u}{\beta_0+\beta_1}e^{-\beta_0 h-\beta_1|z|}J_0(ru)\mathrm{d}u. \tag{15}$$

$$R_2=\sqrt{x^2+y^2+(h+z)^2}. \tag{16}$$

$$E_a=-\frac{j\omega\mu I\mathrm{d}x}{4\pi}\left[\frac{e^{jk_0R_1}}{R_1}-\frac{e^{jk_0R_2}}{R_2}+2\int_0^\infty\frac{u}{\beta_0+\beta_1}e^{-\beta_0(z+h)}J_0(ru)\mathrm{d}u\right]. \tag{17}$$

$$E_e=-\frac{j\omega\mu I\mathrm{d}x}{4\pi}\int_0^\infty\frac{u}{\beta_0+\beta_1}e^{-\beta_0 h-\beta_1|z|}J_0(ru)\mathrm{d}u. \tag{18}$$

It is to be noted that the model presented above has been used to calculate the sheath voltage and current, despite that there are standards and guides [16–19] for the calculation. The main difference between the proposed model and the methods given in the standards/guides lies in the calculation of the induced voltages from the current of nearby circuits. The methods used in the standards/guides simplified the Carson formula/the Pollaczek's formula whilst the proposed model did not. These formulae originate from the principle of communication, and they can be derived from Maxwell's equations, the theory of electric dipole [20] and Sommerfeld integral [21]. In other words, the proposed model for calculating the exact maximum electrical length is based on first principles.

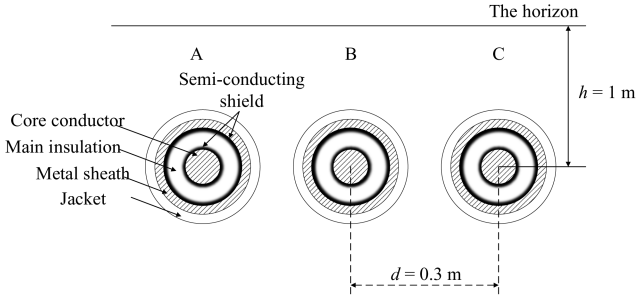

Fig. 8 *Configuration of typical 110 kV HV cable circuit with horizontal laying*

Table 1 Parameters of cross-sectional structure of the cable

	Structure	Outer radius, mm
1	core conductor (copper)	17.0
2	inner semiconductor (nylon belt)	18.4
3	main insulation (ultra-clean XLPE)	34.4
4	outer semiconductor (super-smooth semi-conductive shielding material)	35.4
5	water-blocking layer (semiconductor)	39.4
6	metal sheath (aluminium)	43.9
7	jacket (PVC)	48.6

4 Calculation of the maximum electrical length of a cable section

As the maximum electrical length of a cable section is governed by the maximum permissible standing voltage, the sheath voltages need to be calculated with different bonding methods.

4.1 Maximum electrical length of the cable section under normal operational conditions

4.1.1 Single-point bonding: As there is only one direct earthing point of the metal sheath, the sheath current I_m is negligible. The electromotive force induced by the line itself can be calculated by (8) and the electromotive force induced from nearby circuits can be calculated by (17) or (18).

To make the results more intuitive, calculation has been carried out for a typical 110 kV HV cable circuit with horizontal laying, as shown in Fig. 8. All cable core conductors have a cross section of 800 mm^2, with a rated load of 1050 A. The parameters of cable's cross-sectional structure are shown in Table 1, and the results of the calculation of induced voltage per kilometre on the metal sheath of each cable phase are shown in Table 2.

As Table 2 shows, the laying environment makes little difference to the induced voltage on the metal sheath, the maximum voltage appeared on the phase B cable, and the maximum length of the cable section can be calculated by dividing the permissible sheath standing voltage by this value. Based on a maximum permissible sheath voltage of 300 V under normal conditions [5], the maximum electrical length of a cable section is 2.21 km.

4.1.2 Middle-point bonding: As discussed, the only direct earthing point is at the middle of this cable section. A single-point bonding cable section is like a half of a middle-point bonding cable section. The directly earthed cable circuit has the same form as two symmetrical single-point bonded cable sections, as shown in Fig. 3. Therefore, the maximum sheath voltage calculation of a cable with middle-point bonding is the same as for single-point bonding. However, as there are two single-point bonding sections in a middle-bonding cable, the maximum electrical length of the middle-point bonding cable section is 4.42 km.

Table 2 Induced voltage per kilometre on the metal sheath (V/km)

Laying environment	Cable phase		
	A	B	C
air	135.112	135.444	135.112
earth	135.111	135.444	135.111

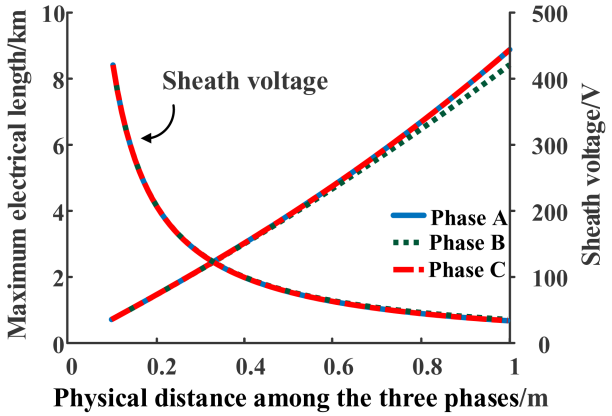

Fig. 9 *Results of the influence of physical distance among the three phases*

4.1.3 Further study: The distance between each cable phase (A, B, and C) in Fig. 8 is $d = 0.3$ m. The influence of the physical distance among the three phases on the sheath voltage can be calculated by setting d as an independent variable. For this work the variation in range is from 0.1–1 m. The results are shown in Fig. 9.

There are two clusters of curves in Fig. 9, the curve which has an upward trend as physical distance increases shows the change in maximum electrical length with change in physical distance d among the three phases: left-hand axis. The curve cluster, which declines with increasing distance between cables, represents the sheath voltage in relation to the physical distance d among the three phases, right-hand axis. The results show a significant influence on both characteristics of the physical distance among the three phases. The greater the physical distance among the three-phase cables, the greater the maximum electrical length of the cable section. If the three-phase cables are laid in the air in a triangular formation, i.e. positioned so that the cable centres are equidistant, the resulting curves are almost the same as those in Fig. 9, and the numerical differences are also small. The influence of depth of burial of cable, h, and the load rating, as analysed and discussed below, also show similar results to that for the horizontal laying in the earth and the equilateral triangle laying in the air.

In this study the buried depth h is set as the independent variable: the variation in depth is from 0.1–10 m. The influence of h can be shown in Fig. 10, the downward trending curve cluster represents the change in maximum electrical length with the buried depth h, left-hand axis. The rising curve cluster represents the variation in sheath voltage with the cable depth h, right-hand axis. The results show the influence of the cable depth is insignificant. Burying cables more deeply would not increase the maximum electrical length of the cable section.

The load current in the cable is another factor influencing the maximum electrical length of the cable section. Therefore, the load rate is set as an independent variable in this study: the variation range is from 10–150% of rated load. As shown in Fig. 11, not surprisingly, the sheath voltage increases linearly with the load rate. There is no need to compare the relationship between the maximum electrical length and load rate, because the maximum electrical length of the cable section has to be designed under the load rate of 100%. Excessive load will lead to not only an increase in cable temperature but also an increase in the sheath voltage at the isolated end. Operators will be aware of this danger when operating above the rated current.

4.2 Choices of sheath protector considering short-circuit fault conditions

Sheath protectors, or sheath voltage limiters, have been introduced to protect sheath sectionalising insulators and cable jackets from overvoltage. There are three main types of sheath protector: metal oxide arresters (MOAs), silicon carbide (SiC) blocks, and spark gaps. The MOAs are the most widely used, as they have a number of advantages over older limiter designs, i.e. those incorporating SiC and/or spark gaps. The main criterion for selecting sheath protectors is the sheath to earth voltage, to conform with safety standards the sheath protectors should be conducting when the sheath voltage exceeds 300 V.

4.2.1 Single-point bonding: If a short-circuit fault occurs in a single-point bonding cable section, the fault current would be very high and the voltage between the two ends of the sheath protector would also be very high. However, most of the MOAs on the existing market cannot withstand discharge currents exceeding 20 kA, so that a lot of incidences of MOAs exploding have been reported. For economic considerations, as the cost of replacing a MOA is much cheaper than the fault repair of a HV cable, the current capacity is not always the first consideration in selecting the protection device.

4.2.2 Middle-point bonding: The criterion for selecting sheath protectors for middle-point bonding cables is the same as single-point bonding cables. While there is one more MOA for a middle-point bonding cable section, if the current capacity is too low, the two MOAs may be overloaded at the same time and may also explode.

5 Economic comparison for each bonding method

The total cost of construction of an HV cable system mainly consists of the cost of cable body, the cost of cable terminal, the cost of cable joints, the cost of cable channel and the cost of parallel GCC. No matter which bonding method has been chosen, the costs of cable body, the cable terminal, and the cable channel are the same. Therefore, the economic difference among different methods mainly depends on the cost of cable joints and the cost of GCC. The unit prices of GCC and HV cable joints are shown in Table 3.

Let C_C be the total cost of GCC and cable joints using the cross-bonding method, let C_M be the total cost of GCC and cable joints using middle-point bonding method, and C_S the total cost of GCC and cable joints using single-point bonding method. Let x be the unit price of the cable joint, and L the length of the cable. As there are six cable joints in a major cross-bonding section with no GCC, three cable joints in a middle-point bonding section with GCC, and no cable joint in a single-point bonding section with GCC, the values of C_C, C_M, C_S can be represented in (19)–(21), respectively. Using the data in Table 3, the results of the comparison of the three cable jointing methods is shown in Figs. 12*a–c*

$$C_C = 6x. \tag{19}$$

$$C_M = 3x + 146L. \tag{20}$$

$$C_S = 146L. \tag{21}$$

For a major cable section with a length of 1200–2210 m, the bonding techniques with GCC (middle-point bonding and single-point bonding) are more expensive than the cross-bonding technique. The specific economic comparison of each bonding technique is shown in Table 4. Only when the 220 kV cable (2500 mm^2) length is between 1200 and 1644 m, does the single-point bonding and middle-point bonding have better economic value, otherwise, cross-bonding is more economic.

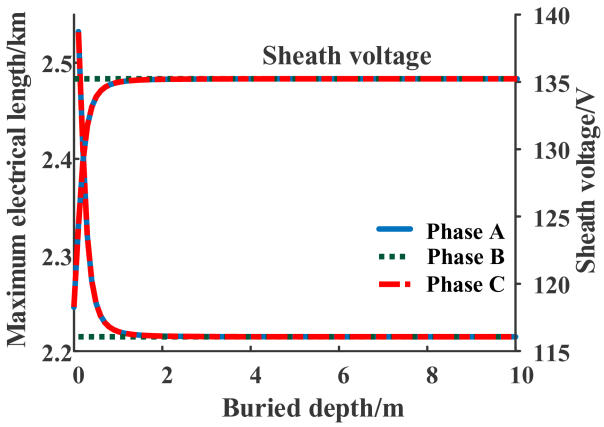

Fig. 10 *Results of influence of buried depth*

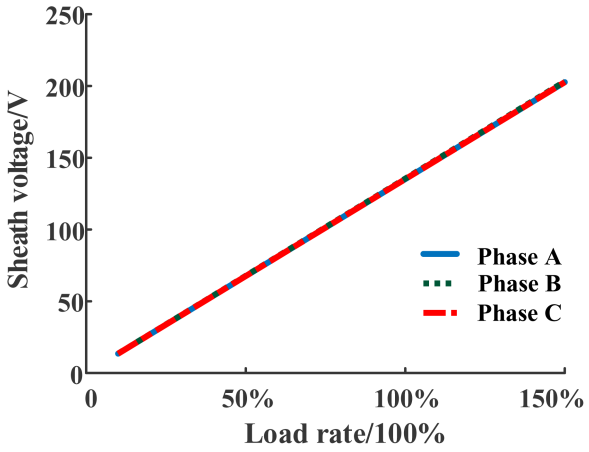

Fig. 11 *Results of the influence of load rate*

Table 3 Unit prices of GCC and HV cable joint

	Object	Unit price[a]
1	GCC	¥ 146/m
2	110 kV cable joint (<800 mm^2)	¥ 14,000
3	110 kV cable joint (800 mm^2)	¥ 15,000
4	220 kV cable joint (2500 mm^2)	¥ 80,000

[a]The data comes from the power company receiving a quote from the power equipment manufacturer.

6 Practical case study of a lengthened cable section

Based on the actual circuit path and the expected load growth, a cable circuit was designed with the length of 1465 m: the cross section of the selected 220 kV cable core conductor is 2500 mm^2 for the rated load of 1860 A. According to the results of the economic comparison of the different bonding methods, shown in Table 4, middle–point bonding and single–point bonding have better value in this case. The middle-point bonding was finally selected. The parameters of cross-sectional structure of this cable are shown in Table 5, and the 220 kV cable circuit is shown in Fig. 13. The cable circuit is now laid in a tunnel in Nanjing, China.

Since the GCC is laid around the cable body, there is an induced voltage on the GCC; because the two ends of GCC are directly grounded, sheath circulating current flows along the GCC. Ideally the GCC should be laid with phase transposition separating the cable into equal lengths. However, this is not always practically possible. In this case, the actual laying configuration is shown in Fig. 14. It was calculated that the maximum sheath voltage is at terminal 2 of the phase C cable, with a magnitude of 161.50 V. If the GCC was not adopted, the maximum sheath voltage would be at cable terminal 2 of both phase C and phase A, with a magnitude of 154.64 V. Therefore, the GCC cannot reduce the maximum

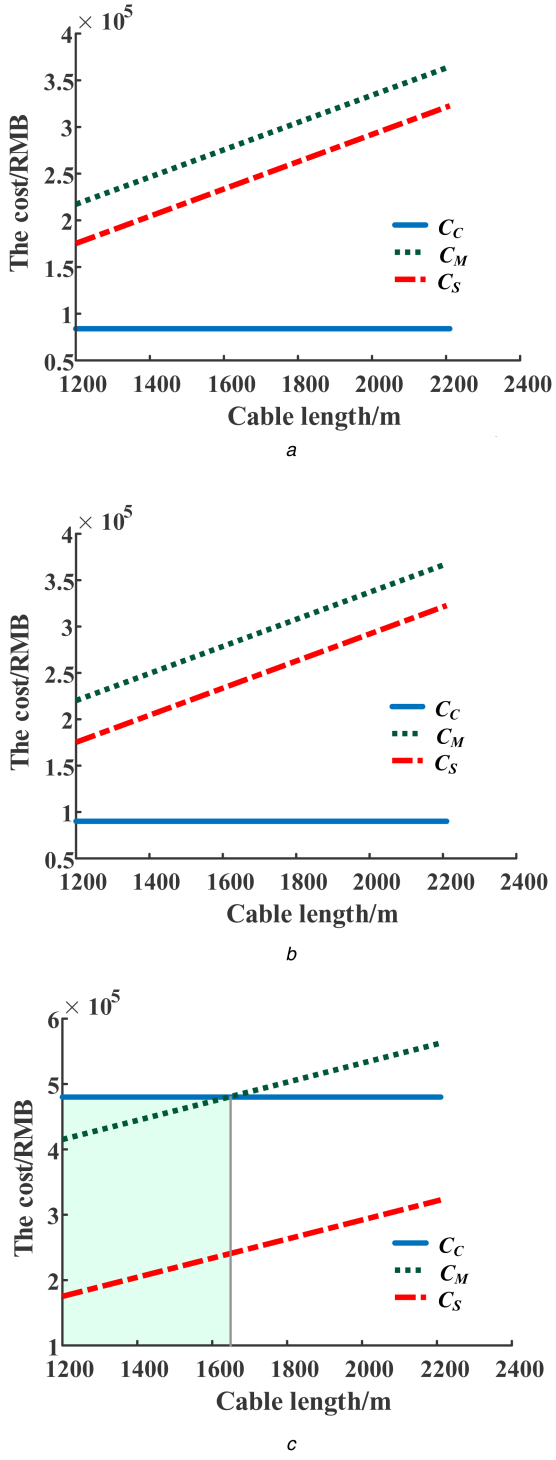

Fig. 12 *Economic comparison for each bonding method*
(a) 110 kV cable joint (<800 mm^2), ***(b)*** 110 kV cable joint (800 mm^2), ***(c)*** 220 kV cable joint (2500 mm^2)

sheath voltage under normal conditions. In fact, the GCC is installed mainly to create a return path for fault currents during grounding faults. It is also to be noted that the metal sheath of power cables is usually designed to complete the fault current loop [22]. An additional return path may not be necessary under most instances.

The 220 kV cable has been operating normally since November 2017. The operational data and calculation results are shown in Table 6, as the load current is low, the sheath voltage and the GCC current are also low. As can be seen form the data presented, the actual operational data and the calculation results are in good agreement.

Table 4 Economic comparison of each bonding method

HV cable	Cable length Better economical bonding method	
	1200–1644 m	1644–2210 m
110 kV cable joint (<800 mm^2)	cross-bonding	cross-bonding
110 kV cable joint (800 mm^2)	cross-bonding	cross-bonding
220 kV cable joint (2500 mm^2)	middle-point bonding single-point bonding	cross-bonding

Table 5 Parameters of cross-sectional structure of the 220 kV cable

	Structure	Outer radius, mm
1	core conductor (copper)	30.6
2	inner semiconductor (nylon belt)	32.0
3	main insulation (ultra-clean XLPE)	60.9
4	outer semiconductor (super-smooth semi-conductive shielding material)	61.9
5	water-blocking layer (semiconductor)	63.9
6	metal sheath (aluminium)	68.7
7	jacket (PVC)	73.7

7 Discussion

Cable failure statistics indicate that the failure rate of cable joints is higher than that for cable bodies. By lengthening the cable section, the number of joints will be reduced, which is expected to result in improved reliability, as joint failures accounted for majority of the cable circuit faults. There may require to be different condition diagnosis methods for the lengthened cable, but the condition-based maintenance strategy stays the same in essence. The inspection and test cycles may be extended due to the reduction of the number of cable joints, though the content of the inspection and test will remain the same.

8 Conclusion

In order to reduce failure rate and improve the reliability of HV cable systems, this paper has studied the possibility of lengthening a HV cable section and reducing the number of cable joints. This has included an evaluation of the cross bonding method against the single-point bonding and middle-point bonding. The limitations for the maximum electrical length of the cable section have been analysed through the sheath voltage calculation and an economic comparison. From the results it can be concluded that

(i) The traditional 500-m minor section could be lengthened to 2.21 km by using the single-point bonding method, based on calculations using a typical HV cable.
(ii) Simulation results indicate that the physical distance between each phase cable has a great influence on the sheath voltage. The maximum electrical length of the cable section can be lengthened by increasing the physical distance among the three phases. The influence of the depth at which the cable is buried is insignificant, and the sheath voltage increases linearly with the load current applied.
(iii) The results of economic comparison showed that there is a cable section length range for which single-point bonding or middle-point bonding has better economic value than cross-bonding.
(iv) Based on the theoretical study, a 220-kV cable section has been lengthened to 1465 m in practice, which provided better economic value. This cable was commissioned in 2017 and has been in normal operation since then. The safe and consistent operation of the lengthened cable section over the intervening period validates the feasibility of the proposed method.

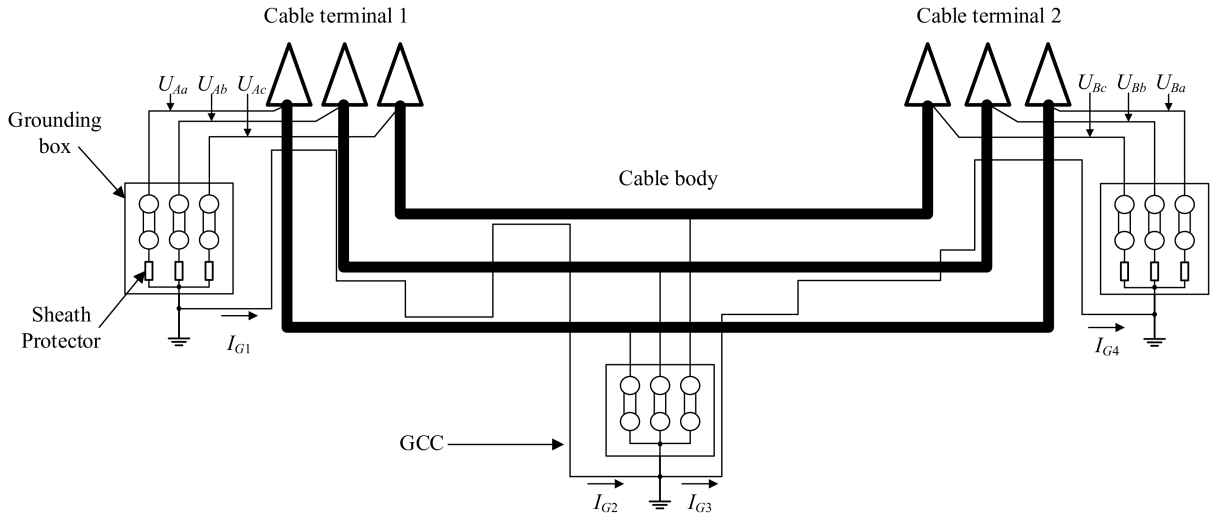

Fig. 13 *Configuration of the 220 kV cable circuit*

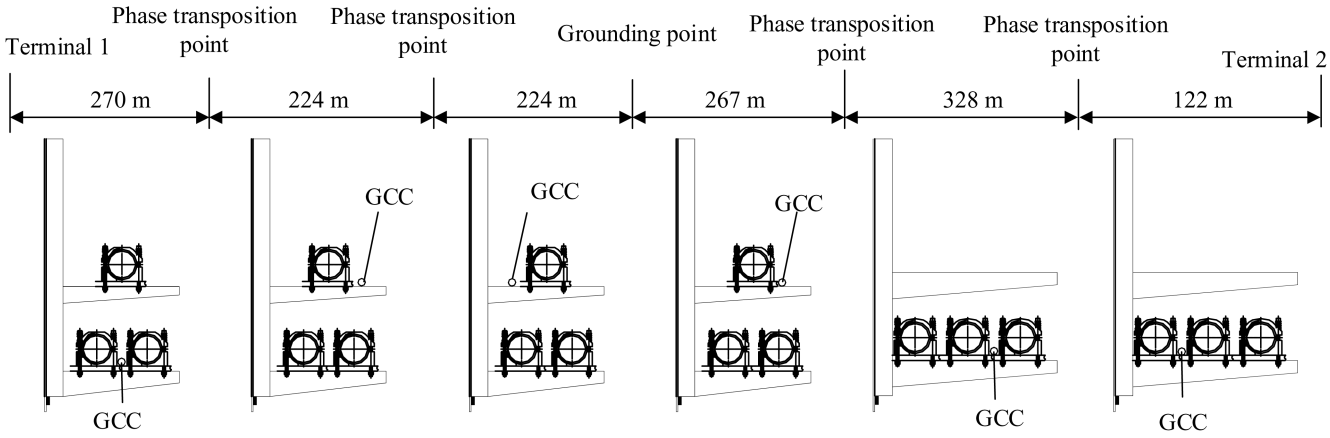

Fig. 14 *Practical laying configuration of the 220 kV cable*

Table 6 Comparison of actual operational data and calculation results for the 220 kV cable

	Operation data[a]	Calculation results	Error, %
sheath voltage (U_{Aa})	3.01 V	2.98 V	1.00
sheath voltage (U_{Ab})	3.87 V	3.58 V	7.49
sheath voltage (U_{Ac})	3.03 V	2.99 V	1.32
sheath voltage (U_{Ba})	3.11 V	3.03 V	2.57
sheath voltage (U_{Bb})	2.89 V	2.88 V	3.46
sheath voltage (U_{Bc})	3.15 V	3.03 V	3.81
GCC current (I_{G1})	0.25 A	0.24 A	4.00
GCC current (I_{G2})	0.25 A	0.24 A	4.00
GCC current (I_{G3})	0.49 A	0.48 A	2.04
GCC current (I_{G4})	0.49 A	0.48 A	2.04

[a]The load current is 40.3 A when measurements were taken and this value was used for the calculations.

9 References

[1] Zhou, C., Yi, H., Dong, X.: 'Review of recent research towards power cable life cycle management', *High Volt.*, 2017, **2**, (3), pp. 179–187

[2] Rahman, D., Mohsen, G., Mohammad, D.: 'Fault location in power distribution network with presence of distributed generation resources using impedance based method and applying π line model', *Energy*, 2018, **159**, (9), pp. 344–360

[3] Marzinotto, M., Mazzanti, G.: 'The feasibility of cable sheath fault detection by monitoring sheath-to-ground currents at the ends of cross-bonding sections', *IEEE Trans. Ind. Appl.*, 2015, **51**, (6), pp. 5376–5384

[4] Tang, Z., Zhou, W., Zhao, J., *et al.*: 'Comparison of the Weibull and the crow-AMSAA model in prediction of early cable joint failures', *IEEE Trans. Power Deliv.*, 2015, **30**, (6), pp. 2410–2418

[5] Das, S., Majumder, R., Singh, S.: 'Cable joint installation time optimization', *IEEE Trans. Dielectr. Electr. Insul.*, 2017, **24**, (6), pp. 3959–3965

[6] Peixoto, C.D., Filho, E.K., Louredo, N.H.G.R.: 'Statistics of failures on underground high voltage power cables in Brazil'. CIGRE 2010, Paris, France, 2010, pp. 1–7

[7] Lebert, A.W., Fischer, H.B., Biskeborn, M.C.: 'Cable design and manufacture for the transatlantic submarine cable system', *Bell Syst. Tech. J.*, 1957, **36**, (1), pp. 189–216

[8] Montanari, G.C., Morshuis, P., Zhou, M., *et al.*: 'Criteria influencing the selection and design of HV and UHV DC cables in new network applications', *High Volt.*, 2018, **3**, (2), pp. 90–95

[9] Wang, X., Wang, C., Wu, K., *et al.*: 'An improved optimal design scheme for high voltage cable accessories', *IEEE Trans. Dielectr. Electr. Insul.*, 2014, **21**, (1), pp. 5–15

[10] Urquhart, A.J., Thomson, M.: 'Series impedance of distribution cables with sector-shaped conductors', *IET Gener. Transm. Distrib.*, 2015, **9**, (16), pp. 2679–2685

[11] Yang, F., Zhu, N., Liu, G., *et al.*: 'A new method for determining the connection resistance of the compression connector in cable joint', *MDPI Energies*, 2018, **11**, (7), Article ID: 1667

[12] Yang, F., Cheng, P., Luo, H., *et al.*: '3-D thermal analysis and contact resistance evaluation of power cable joint', *Elsevier Appl. Thermal Eng.*, 2016, **93**, pp. 1183–1192
[13] Zhou, C., Song, X., Michel, M., *et al.*: 'On-line partial discharge monitoring in medium voltage underground cables', *IET Sci. Meas. Technol.*, 2009, **3**, (5), pp. 354–363
[14] Lu, G., Wu, G., Xiong, J., *et al.*: 'Sensitivity analysis of cable oscillating wave test system on multi-source defects diagnostics'. CIRED Int. Conf. & Exhibition on Electricity Distribution, Glasgow, UK, 2017, pp. 424–427
[15] Sheng, B., Zhou, C., Hepburn, D., *et al.*: 'Partial discharge pulse propagation in power cable and partial discharge monitoring system', *IEEE Trans. Dielectr. Electr. Insul.*, 2014, **21**, (3), pp. 948–956
[16] CIGRE TB 283: 'Special bonding of high voltage power cables', 2005
[17] IEEE Std 575™-2014: 'IEEE guide for bonding shields and sheaths of single-conductor power cables rated 5 kV through 500 kV', 2014
[18] IEEE Std 635™-2003: 'IEEE guide for selection and design of aluminum sheaths for power cables', 2003
[19] GB 50217-2007: 'Code for design of cables of electric engineering', 2007
[20] Vaughan, R., Bachanderson, J.: '*Channels, propagation and antennas for mobile communications*' (IET Electromagnetic Waves Series 50, London, UK, 2003)
[21] Sommerfeld, A.: '*Partial differential equations in physics*' (Academic Press Inc, Cambridge, MA, USA, 1949)
[22] McAllister, D.: 'Theory, design and principles to all cable types', in '*Electric cables handbook*' (Blackwell Science., Oxford, UK, 1982, 3rd edn.), pp. 1–204